ARTICLE
Journal of Cellular Biochemistry 115:826–838 (2014)

Journal of Cellular Biochemistry

Human Keloid Cell Characterization and Inhibition of Growth with Human Wharton's Jelly Stem Cell Extracts

Chui-Yee Fong, Arijit Biswas, Arjunan Subramanian, Akshaya Srinivasan, Mahesh Choolani, and Ariff Bongso*

Department of Obstetrics and Gynaecology, Yong Loo Lin School of Medicine, National University Health System, National University of Singapore, Kent Ridge, Singapore 119228, Singapore

ABSTRACT

Keloids are firm rubbery growths that grow beyond the boundaries of human wounds and their treatment has met with limited success. Their properties and growth behavior have not been properly characterized and it has been suggested that a benign neoplastic stem cell-like phenotype in an altered cytokine microenvironment drives their uncontrolled cell proliferation. Modification of the stem cell niche may be an attractive approach to its prevention. We studied the growth behavior, stemness, and tumorigenic characteristics of keloid cells in prolonged culture. Since human Wharton's jelly stem cells (hWJSCs) secrete high levels of cytokines and have anti-tumorigenic properties we explored its role on the inhibition of keloid growth in vitro. Keloid cells grew readily in both adherent and sphere culture and expressed high levels of mesenchymal CD and tumor-associated fibroblast (TAF) markers up to passage 10. When they were exposed to repeat doses of hWJSC conditioned medium (hWJSC-CM) and lysate (hWJSC-CL) every 72 h up to 9 days their growth was inhibited with a reduction in CD and TAF marker expression. On Days 3, 6, and 9 treated keloid cells showed linear decreases in cell proliferation (BrdU), increases in Annexin V-FITC and TUNEL-positive cells, interruptions of the cell cycle and inhibition of migration in scratch-wound assays. Immunocytochemistry and qRT-PCR confirmed a significant downregulation of TAF and anti-apoptotic-related gene (SURVIVIN) expression and upregulation of autophagy-related (BAX, ATG5, ATG7, BECLIN-1) gene expression. The results suggest that hWJSCs or molecules secreted by them may be of therapeutic value in the treatment of keloids. J. Cell. Biochem. 115: 826–838, 2014.

KEY WORDS: CONDITIONED MEDIUM; GROWTH INHIBITION; HUMAN WHARTON'S JELLY STEM CELLS; KELOIDS; LYSATE

Keloids are fibro-proliferative benign scars unique to the human that show aggressive dermal growth beyond the boundaries of the original margins of wounds. Morphologically they are firm, rubbery, claw-like growths with shiny surfaces that generate pain, pruritis, and contractures and are a cosmetic and psychological burden to patients. They are essentially slow-growing neoplasms characterized by the benign proliferation of fibroblasts due at least in part to altered cytokine profiles [Moon et al., 2008]. Wounds can end up in keloids after burns, ear-piercing, trauma, infection, vaccination, surgery, burns and even spontaneously [Mogili et al., 2012]. The current treatments for keloids have not produced conclusive results [Gauglitz et al., 2011; Gauglitz, 2013].

Very little is known about the pathogenesis of keloids which has influenced the lack of proper treatment strategies and one important hurdle reported by Blit and Jeschke [2012] was the lack of proper characterization of keloids in terms of its nature and properties. Some of the predisposing factors for keloid formation include (1) the severity of inflammation, immune and fibrogenic response to wounds, (2) high levels of TGF-β at the site of injury, (3) interactions between keratinocytes and fibroblasts, (4) mast cells as a source of pro-inflammatory mediators, (5) extracellular matrix (ECM) degradation by matrix metalloproteinases (MMPs), (6) delayed apoptosis of myo-fibroblasts in wound beds, (7) sebum interacting with T-cells on the skin surface leading to an inflammatory reaction, and (8) altered angiogenic balance [Gauglitz et al., 2011; Iqbal et al., 2012; Mogili et al., 2012].

It has been reported that primary fibroblast-like cell populations obtained from various tissues contain mesenchymal progenitor and stem cells [Sudo et al., 2007]. These observations led Moon et al. [2008] to postulate that the fibroblasts in the keloid dermis were

All authors have no conflicts of interests.

Grant sponsor: Academic Research Fund; Grant sponsor: National University of Singapore (AcRF-NUS); Grant number: R-174-000-129-112; Grant sponsor: National Medical Research Council (NMRC); Grant number: R-174-000-131-213.

*Correspondence to: Prof. Ariff Bongso, Department of Obstetrics and Gynaecology, Yong Loo Lin School of Medicine, National University Health System, Kent Ridge, Singapore 1190741. E-mail: obgbongs@nus.edu.sg

Manuscript Received: 9 November 2013; Manuscript Accepted: 18 November 2013

Accepted manuscript online in Wiley Online Library (wileyonlinelibrary.com): 22 November 2013

DOI 10.1002/jcb.24724 • © 2013 Wiley Periodicals, Inc.

actually multipotent stem cells that were being maintained in a proliferating and undifferentiated state by a specific local cytokine microenvironment in wounds. Based on this hypothesis these workers successfully isolated, cultured, and identified fibroblasts with stemness properties in adult keloid tissue samples. Their keloid-derived mesenchymal-like stem cells (KMLSCs) expressed the MSC markers CD13, CD29, CD44, CD90, fibronectin, and vimentin and differentiated into osteogenic, chondrogenic, adipocytic, smooth muscle, endothelial, and neuronal lineages. Later, Zhang et al. [2009] showed that altered niches in keloids which were predominantly inflammatory, contributed to the acquirement of a benign tumor-like stem cell phenotype of keloid-derived precursor cells (KPCs). These cells had uncontrolled self-renewal and increased proliferation supporting the argument that in vivo modification of the stem cell niche may be a form of potential therapy for keloids.

It was suggested that the most promising area of research toward effective keloid therapy lied in stem cells [Blit and Jeschke, 2012]. Treatment of murine skin defects with human bone marrow MSCs (hBMMSCs) resulted in scarless healing in 14 days [Mansilla et al., 2005]. hBMMSCs secrete a variety of cytokines and growth factors that have anti-fibrotic properties, including hepatocyte growth factor (HGF) and IL-10 (10–12). The anti-fibrotic properties of IL-10 were further confirmed recently by Kieran et al. [2013]. Unfortunately, hBMMSCs have short-lived stemness properties in vitro and the frequency, proliferation efficiency and differentiation capacities of hBMMSCs decrease with age [Rao and Mattson, 2001]. Autologous sources require painful harvest with the patient running the risk of infection and morbidity while allogeneic sources are not immunoprivileged and have to be expanded to obtain adequate numbers for treatment.

We have studied a primitive MSC from the human umbilical cord Wharton′s jelly (hWJSCs) that has uniquely different properties from hBMMSCs and other MSCs. [Fong et al., 2010, 2011, 2012; Gauthaman et al., 2011, 2012a; Bongso and Fong, 2013]. The advantages of hWJSCs over other MSCs include their (i) painless harvest, availability in large numbers, high proliferation rate, and short population doubling time, (iii) prolonged stemness properties in vitro, and (iv) hypoimmunogenicity and tolerance in donor settings [Chao et al., 2008; Seshareddy et al., 2008; Troyer and Weiss, 2008; La Rocca et al., 2009; Fan et al., 2011; Prasanna and Jahnavi, 2011]. Given their rapid multiplication they can be scaled up in large numbers for clinical application. hWJSCs are safe and do not induce tumor formation in laboratory animals [Fan et al., 2011; Gauthaman et al., 2012a], non-human primates [Wang et al., 2012], and in human transplantation settings [Chen et al., 2012; Wu et al., 2013b].

Paradoxically, several independent groups have reported that hWJSCs have unique anti-tumorigenic properties [Rachakatla et al., 2007; Ayuzawa et al., 2009; Ganta et al., 2009; Maurya et al., 2010; Sun et al., 2010; Ma et al., 2011; Chao et al., 2012; Fonseka et al., 2012; Gauthaman et al., 2012b, 2013; Liu et al., 2013; Wu et al., 2013a]. Such anti-tumorigenic properties were related to the expression of high levels of tumor-suppressor and pro-apoptotic genes observed during comparative transcriptome profiling of hWJSCs with other stem cell types [Nekanti et al., 2010; Fong et al., 2011]. hWJSC extracts (hWJSC-CM and hWJSC-CL) also inhibited the growth of breast adenocarcinoma, ovarian adenocarcinoma and osteosarcoma cells in vitro and attenuated or abolished the growth of breast tumors in xenograft animal models [Rachakatla et al., 2007; Ayuzawa et al., 2009; Ganta et al., 2009; Gauthaman et al., 2012a, 2013].

These unique properties of hWJSCs were attributed to their umbilical cord origin which embryologically lies in between embryonic and adult tissues on the human developmental map [Pappa and Anagnou, 2009]. During early human development MSCs migrate from the aorta-gonad-mesonephros (AGM) of the embryo through the umbilical cord to the placenta and then migrate back again through the umbilical cord to home in the liver and bone marrow of the fetus [Wang et al., 2008]. During their migration these primitive stem cells get trapped in the gelatinous Wharton′s jelly of the umbilical cord, reside there and acquire unique characteristics in their new environment [Taghizadeh et al., 2011]. Yang and Chao [2013] hypothesized that hWJSCs in the umbilical cord play a natural role in the fetal defense against cancer.

Interestingly, abdominal hernias in newborn infants have been successfully treated by attaching the infant′s own umbilical cord with its Wharton′s jelly to the hernia with no ensuing scar and keloid formation [Lorenz et al., 1992; Estes et al., 1993]. Thus, primitive hWJSCs which are not exposed to the insults of the adult environment and because of their anti-tumorigenic properties may have a role to play in the absence of scar and keloid formation in the fetus during pregnancy. Since keloid cells resemble and behave like benign tumorigenic cells we explored the role of hWJSCs and its extracts on the inhibition of keloid cell growth in vitro.

MATERIALS AND METHODS

CELL CULTURE

Human Wharton′s jelly stem cells. Ethical approval for the use of human umbilical cords from consenting patients was given by the Institutional Domain Specific Review Board (DSRB), Singapore. hWJSCs were derived and characterized according to our published protocols [Fong et al., 2010]. Umbilical cords were collected in a transport medium (Hank′s Balanced Salt Solution supplemented with antibiotic-antimycotic solution, Invitrogen Life Technologies, Carlsbad, CA), stored at 4°C and processed within 12 h after collection. Each cord was first cut into 2 cm pieces and each of these pieces cut open lengthwise and placed with its inner surface facing down in a 60 mm Petri dish containing an enzymatic solution. The enzymatic solution comprised of 2 mg/ml collagenase type I, 2 mg/ml collagenase type IV, and 100 IU/ml hyaluronidase (Sigma Chemical Co, MO) in DMEM High glucose medium (Invitrogen). The umbilical blood vessels were not removed. The dishes were then incubated at 37°C for 30–45 min to facilitate detachment and loosening of the Wharton′s jelly into the culture medium. The gelatinous Wharton′s jelly was then collected into sterile syringes and passed through hypodermic needles to and fro to separate the hWJSCs. The isolated hWJSCs were cultured in sterile tissue culture flasks [Becton Dickinson (BD) Franklin Lanes, NJ] using hWJSC culture medium comprised of DMEM-high glucose medium supplemented with 20% fetal bovine serum (FBS), 16 ng/ml basic fibroblast growth factor (Millipore Bioscience Research agents, Temecula, CA), 1% non-essential amino acids, 2 mM L-glutamine,

0.1 mM β-mercaptoethanol, 1% insulin-transferrin-selenium, and 1% antibiotic-antimycotic mixture [penicillin (100 units/ml), streptomycin (100 μg/ml), and amphotericin B (0.25 μg/ml)] (Invitrogen). After establishment of confluent monolayers the hWJSCs were detached from the plastic dishes with trypsin-EDTA (TrypLE^{TM} Express, Invitrogen), dissociated, washed, and seeded on 0.1% gelatin-coated tissue culture plates in a basal medium devoid of proteins comprised of DMEM-high glucose, 10% knockout serum replacement (KOSR), 1% L-glutamine and 1% antibiotic-antimycotic mixture (KOSR medium, Invitrogen) for all the experiments of the present study. A protein-free basal medium was used to avoid the artifactual influence of any proteins from the medium and to take advantage of the various proteins released by the hWJSCs.

Human foreskin fibroblast cells. Human foreskin fibroblasts (CCD-112sk) (abbreviated as CCD) were obtained from the American Type Culture Collection (ATCC, MD) to act as controls and ethical approval for their use was given by the National University of Singapore Institutional Review Board (NUS-IRB). The commercial frozen CCDs were thawed and cultured in sterile tissue culture flasks (BD) in DMEM-high glucose medium supplemented with 10% FBS, 2 mM L-glutamine and antibiotic-antimycotic mixture (Invitrogen).

Human keloid cells. Ethical approval for the use of keloid tissues from consenting patients was also given by the Institutional Domain Specific Review Board (DSRB), Singapore. The keloid tissues were collected in HBSS (Invitrogen) and adherent and sphere cultures were set up according to the method of Zhang et al. [2009]. The sample was cut into 2 to 3 cm pieces, washed with fresh HBSS and then exposed to 3 mg/ml dispase (Invitrogen) overnight at 4°C. After overnight incubation, the epidermis was manually removed and the dermis minced into small pieces (1 mm^3). The pieces were placed in collagenase type I (4 mg/ml) (Sigma) and incubated at 37°C in a 5% CO_2 in air atmosphere for 2 h. After enzymatic digestion the cell suspension was centrifuged at 300*g* for 5 min and the cell pellet re-suspended in DMEM low glucose (Invitrogen) supplemented with 10% FBS (Biochrom AG, Berlin, Germany). The cell suspension was then filtered through a 70 μm cell strainer [Becton Dickinson (BD)], centrifuged at 300*g* for 5 min, supernatant discarded, and the cells cultured under two different conditions (adherent and sphere culture).

Adherent Culture. Keloid cells were re-suspended in keloid medium comprised of DMEM supplemented with 10% FBS, 100 IU/ml penicillin, 100 μg/ml streptomycin, 2 mM L-glutamine, 100 mM non-essential amino acids (NEAA), 550 μM 2-mercaptoethanol (Invitrogen) and seeded into 100 mm plastic tissue culture Petri dishes (BD). The dishes were incubated at 37°C in a 5% CO_2 in air atmosphere and when they attached to the plastic dishes their morphology and growth were monitored daily and photographed under inverted phase contrast optics.

Sphere Culture. Keloid cells were re-suspended in a combination of equal parts (v/v) of DMEM-low glucose and Ham′s F12 (Millipore Bioscience Research Agents), and then supplemented with 40 ng/ml fibroblast growth factor-2 (FGF-2) (Millipore), 20 ng/ml, epidermal growth factor (EGF) (MiltenyI Biotech Asia Pacific Pte Ltd), antibiotic/antimycotic mixture (Invitrogen) and then seeded into sterile 6-well plates (BD). The plates were incubated at 37°C in a 5% CO_2 in air atmosphere and when the cells started to produce spheres their morphology and growth were monitored and photographed under inverted phase contrast optics.

PREPARATION OF hWJSC AND CCD CONDITIONED MEDIUM AND LYSATE

hWJSCs and CCDs at passages 3–4 (P3–P4) were grown to 80% confluence in KOSR medium and the medium separated after 72 h as hWJSC conditioned medium (hWJSC-CM) and CCD conditioned medium (CCD-CM), respectively. The conditioned media were filter-sterilized using a 0.22 μm Millex-GP syringe filter (Millipore, Billerica, MA) and the pH and osmolality of the media standardised before use in experiments. Both hWJSC-CM and CCD-CM were diluted 1:1 v/v in KOSR medium and used as 50% hWJSC-CM and 50% CCD-CM for all experiments.

hWJSC and CCD cell-free lysates (hWJSC-CL; CCD-CL) were prepared from early passages of hWJSCs and CCDs (P3–P4) using a mammalian cell extraction kit (BioVision, Mountain View, CA) that contained a protease inhibitor cocktail and dithiothreitol. Briefly, the cultured cells were washed once with phosphate buffered saline that contained no calcium and magnesium (PBS$^{(-)}$), disassociated with trypsin (TrypL^{TM} Express, Invitrogen Life Technologies) and centrifuged at 500*g* for 5 min to obtain a cell pellet. The pellet was re-suspended in 100 μl of the cell lysis buffer provided with the kit and pipetted up and down several times and then incubated in ice for 15 min. The contents were then centrifuged at 12,000*g* for 5 min (Eppendorf, Germany) and the clear supernatant (cell-free lysate) separated and stored at −80°C until use. The hWJSC-CL was diluted in KOSR medium to yield a total protein content of 15 μg/ml which was measured using a Nanodrop^{TM} spectrophotometer (Nanodrop Technologies, Wilmington, DW).

EXPOSURE OF KELOID CELLS TO hWJSC-CM AND hWJSC-CL

Experimental design. Adherent cultures of keloid cells were separately exposed to hWJSC-CM and hWJSC-CL (treatments). Controls were keloid cultures exposed to similar concentrations of (i) CCD-CM, (ii) CCD-CL, and (iii) keloid medium (untreated control). All dishes were monitored daily for 9 days with changes in culture medium every 3 days, and cells subjected to comparative analyses of morphological changes (inverted phase contrast optics), cell proliferation (BrdU assay), cell cycle behavior (flow cytometry), CD markers (FACS), cell death (Annexin V-PI), TUNEL assay, scratch-wound assay, keratinocyte and TAF markers, and gene expression profiles (qRT-PCR).

Statistically significant differences between the treatment and control arms for all evaluations were carried out using one-way ANOVA with Bonferroni′s multiple comparisons post hoc analysis using the statistical package for Social Sciences (SPSS 13). The results were expressed as mean ± SEM from three different replicates for individual experiments and a value of $P < 0.05$ was considered statistically significant.

Evaluation of keloid cell inhibition. *Cell morphology.* The growth of the keloid cells exposed to treatments and controls were monitored daily for 9 days and images of morphological changes of cell death captured at low and high magnifications using inverted phase contrast optics (Nikon Instruments, Tokyo, Japan).

CD marker analysis. Keloid cells of treatment and control dishes were dissociated into single cells with trypsin, washed in $PBS^{(-)}$ and blocked with 10% normal goat serum (NGS) (Invitrogen) for 30 min to prevent non-specific binding. The cells were then incubated with primary antibodies for a series of CD markers viz., CD14, CD29, CD34, CD44, CD45, CD73, CD90, and CD105 (Biolegend, San Diego, CA) for 1 h followed by incubation with Alexa Fluor® 488 (1:750) secondary antibody (Invitrogen) for 30 min. The cells were finally washed in $PBS^{(-)}$, re-suspended in 10% NGS and filtered using a 70 μm nylon strainer (BD) to remove any cell clumps and analyzed by Fluorescence-activated cell sorting (FACS) using a CyAn™ ADP Analyzer (Beckman Coulter, Fullerton, CA).

Scratch-wound assay. Keloid cell monolayers were exposed to hWJSC-CM in conventional scratch-wound assays [Cory, 2011] to find out whether their cell migration and growth was inhibited. Keloid cells were first seeded at a density of 0.5×10^6 cells in 60 mm Petri dishes (Nalgene NUNC International, Rochester, NY) and monolayers established within 24–48 h. Uniform linear scratches were made on the keloid monolayers vertically from top to bottom in the midline with a 2 ml graduated serological pipette. The cell debris was washed away gently with PBS and the medium of scratched dishes changed to the treatment (hWJSC-CM) and controls (CCD-CM; untreated). The dishes were incubated at 37°C in a 5% CO_2 in air atmosphere for 72 h and cell migration from the edges of the scratches monitored regularly and photographs taken under inverted phase contrast optics until full closure of the vacant areas. Digitized images of at least 5 random fields within the scratches were taken every 24 h using inverted phase contrast optics until 72 h or full closure of the scratches. Markings on the Petri dishes were used as reference points to monitor the same fields every 24 h. The mean ± SEM percentage extent of closure of the scratches at 24, 48, and 72 h were calculated from the digitized images using an image software program [Walter et al., 2010]. Three replicates were carried out for each assay.

Cell proliferation (BrdU assay). Keloid cells for treatment and control arms were cultured in 24 well plates (2×10^4 cells/well) for 9 days and cell proliferation was measured using a bromodeoxyuridine (BrdU) kit (Millipore). The BrdU assay was performed according to the manufacturer's instructions. Briefly, the cells were incubated for 1–24 h with the BrdU solution (10 μM) followed by removal of the medium and incubation for 30 min with the fixing/denaturing solution. Subsequently, the plate was incubated for 1 h with BrdU detection antibody solution followed by three washes with the wash buffer. This was followed by a 30-min incubation with the HRP conjugated secondary antibody solution, three washes with the wash buffer and incubation with the substrate solution for 30 min. The enzymatic reaction was finally stopped and the amount of BrdU was quantified by measuring absorbance at 450 nm using a microplate ELISA reader (μQuant-BioTek, Winooski, VT).

Cell cycle analysis. Cell cycle analysis using flow cytometry of propidium iodide (PI) stained keloid cells, was used to compare the treatments and controls. Briefly, the cells were disassociated with trypsin, washed and fixed with ice-cold 70% ethanol. The fixed cells were stained with 50 μg/ml PI in PBS containing 0.1% TritonX-100 and 50 μg/ml RNAse-A and then analyzed using a flow cytometer (Epics-Altra, Beckman Coulter).

Annexin V-FITC assay. The annexin V-FITC assay was carried out on keloid cells exposed to the treatments and controls to evaluate rates of apoptosis. Briefly, the keloid cells were dissociated with trypsin, washed once with $PBS^{(-)}$ and then with Annexin V binding buffer (1×). The cells were stained with 5 μl Annexin V-FITC at room temperature for 15 min, counterstained with PI (1 μg/ml) and analyzed using a CyAn™ ADP Analyzer.

TUNEL assay. The degree of DNA fragmentation leading to apoptosis in keloid cells exposed to treatments and controls was evaluated with the DeadEnd™ Fluorometric TUNEL System kit (Promega Corp, WI) that detects TdT (terminal deoxynucleotidyl transferase)-mediated dUDP nick-end labeling (TUNEL)—positive cells. Briefly, the keloid cells were disassociated, washed, and fixed with 4% methanol-free formaldehyde solution for 25 min at 4°C followed by addition of Triton X-100 solution for 5 min at 4°C. Labelling of the DNA fragments was carried out by treating the cells with fluorescin-12dUTP and TdT for 1 h at 37°C in a humidified chamber in the dark. The reaction was stopped by the addition of sodium chloride–sodium citrate solution, the cells washed thrice and then stained with PI (1 μg/ml) in PBS containing DNase-free RNase (250 μg/ml) for 15 min at room temperature in the dark. TUNEL positive cells were analyzed under a fluorescence microscope.

Immunocytochemistry and Gene Expression. Immunocytochemistry and quantitative real time polymerase chain reaction (qRT-PCR) were used to evaluate keratinocyte and TAF marker changes and apoptotic and autophagic gene expression in treatments and control dishes to understand changes in behavior of the keloid cells exposed to hWJSC-CM and hWJSC-CL.

For immunocytochemistry, the keloid cells were analyzed for the keratinocyte markers (cytokeratin, involucrin, filaggrin), TAF markers [fibroblast specific protein (FSP), thrombospondin (Tn-C), and VEGF] and autophagy markers (Beclin-1, LC3B) using their respective primary monoclonal and polyclonal antibodies. The keloid cells were washed in PBS and incubated with 4′-6-Diamidino-2-phenylindole (DAPI; 0.5 μg/ml) (Molecular probes, Invitrogen) for 5 min at room temperature, washed again with PBS and then analyzed using fluorescence microscopy.

For qRT-PCR analysis, the total RNA of keloid cells in treatment and control dishes was extracted using TRIzol™ reagent (Invitrogen). RNA quality and quantity were measured using a Nanodrop™ spectrophotometer (Nanodrop technologies) and all samples were treated with DNase-I prior to first strand cDNA synthesis with random hexamers using the SuperScriptTM first strand synthesis system (Invitrogen). Primer sequences were taken from earlier published studies [Gauthaman et al., 2012b]. qRT-PCR analysis was performed with the ABI PRISM 7500 Fast Real-Time PCR System (Applied Biosystems, Foster City, CA) using SYBR green and relative quantification was performed using the comparative CT (2-ΔΔCT) method.

RESULTS

KELOID CELL CHARACTERIZATION

Untreated keloid cells that were not exposed to treatments (hWJSC-CM and hWJSC-CL) attached well to the plastic and became confluent

monolayers with long spindle-shaped fibroblastic morphology (Fig. 1A) and untreated keloid cells in sphere cultures clustered together to form several translucent spheres of different sizes (Fig. 1B). Flow cytometry analysis of keloid cells in adherent and sphere primary cultures showed high level expression of the mesenchymal stem cell (MSC) CD markers CD29, CD44, CD73, CD90, and CD105 (Adherent culture: 94.06 ± 1.08% to 98.38 ± 1.31%; Sphere culture: 81.01 ± 1.17% to 92.48 ± 2.63%) and low level expression for CD14, CD34, and CD45 (Adherent culture: 1.92 ± 0.61% to 23.11 ± 0.89%; Sphere culture: 11.33 ± 0.74% to 19.38 ± 1.04%) (Fig. 1C,D).

Flow cytometry analysis of adherent keloid cells at passages 6 and 10 also showed high level expression of the MSC CD markers CD29, CD44, CD73, CD90, and CD105 (Passage 6: 97.40 ± 1.84% to 98.71 ± 1.06%; Passage 10: 97.37 ± 2.54% to 98.94 ± 1.17%) and low level expression for CD14, CD34 and CD45 (Passage 6: 3.70 ± 0.73% to 11.04 ± 1.14%; Passage 10: 4.67 ± 0.68% to 8.13 ± 0.94%).

Cell cycle and BrDU assays showed normal cell cycles and no significant differences in cell proliferation at passages 3, 6, and 10. Immunocytochemistry of keloid cells at passage 3 showed positive human keratinocyte-related markers (cytokeratin, involucrin, and filaggrin) (Fig. 1E) and TAF markers (FSP, Tn-C, and VEGF) (Fig. 1F).

KELOID CELL INHIBITION BY hWJSC-CM AND hWJSC-CL

Growth morphology and stemness characteristics. The keloid cells of adherent cultures exposed to hWJSC-CM and hWJSC-CL showed decreased cell growth and few to absence of mitotic cell numbers (Fig. 2Ad,e) compared to controls (Fig. 2Aa–c). The MSC-CD markers (CD29, CD44, CD73, CD90, and CD105) of keloid cells in treatment dishes decreased significantly on Day 3 (hWJSC-CM: 74.63 ± 3.48% to 86.66 ± 1.97%; hWJSC-CL: 68.63 ± 4.36% to 78.22 ± 3.97%) compared to controls (Untreated: 94.06 ± 1.08% to 98.38 ± 1.31%; CCD-CM: 96.88 ± 2.07% to 98.86 ± 1.33%; CCD-CL: 98.43 ± 2.76% to 99.79 ± 0.18%) ($P < 0.05$) (Fig. 2B).

After 9 days of treatment the CD markers decreased further (hWJSC-CM: 59.91 ± 4.12% to 76.00 ± 3.22%; hWJSC-CL: 55.45 ± 2.78% to 75.30 ± 3.02%) compared to the controls (Untreated: 95.21 ± 2.06% to 97.13 ± 1.47%; CCD-CM: 92.78 ± 2.86% to 97.28 ± 1.65%; CCD-CL: 96.44 ± 2.33% to 97.80 ± 1.24%) ($P < 0.05$).

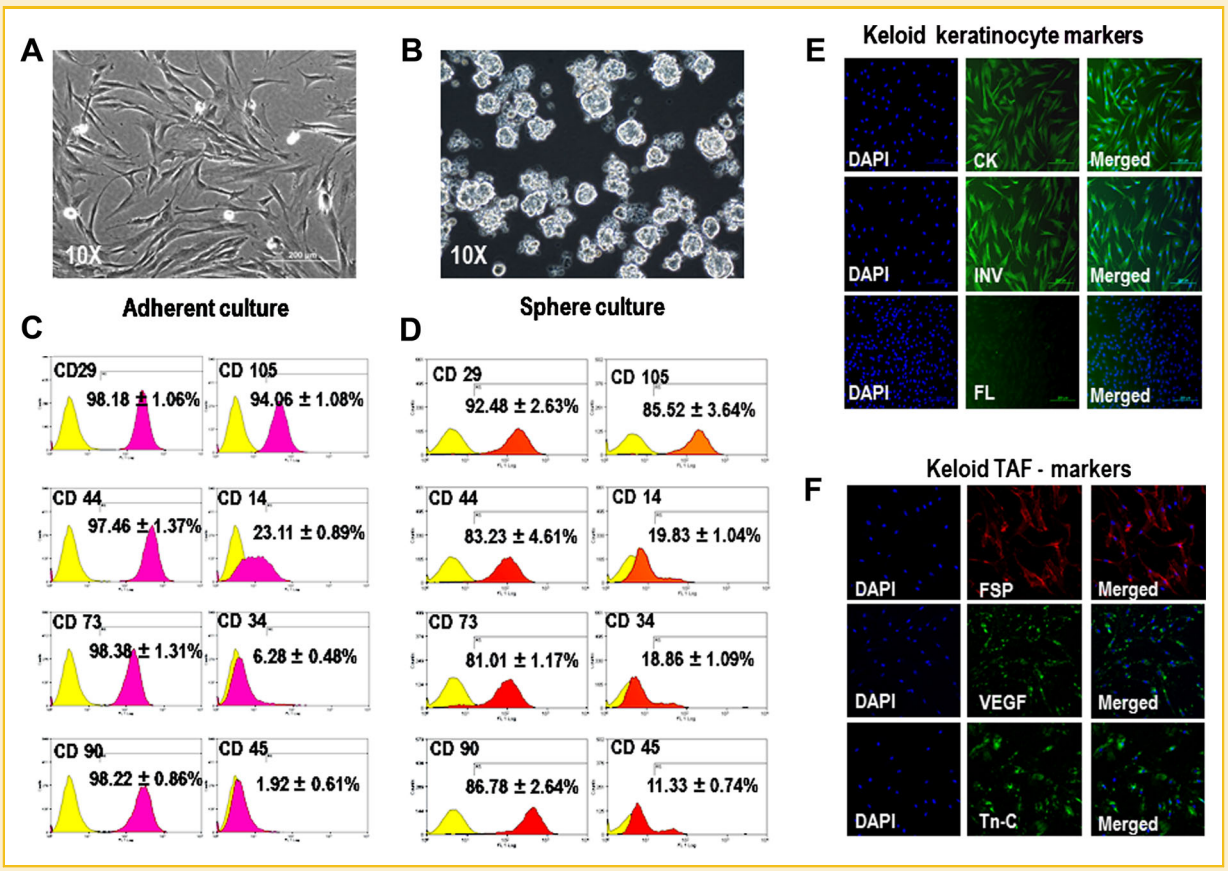

Fig. 1. A: Phase-contrast inverted optical images of human keloid cells attached to plastic and showing spindle-shaped fibroblast-like cell morphology under adherent culture conditions. B: Keloid cells clustered together into spheres in suspension under sphere culture conditions. C: FACS analysis for CD markers of keloid cells in adherent culture and (D) Sphere culture. Data are from three independent experiments and each contour map represents the percentage of FITC-positive cells against unstained controls for each CD marker. E: Immunocytochemistry images of human keloid cells showing positive keratinocyte-related markers [cytokeratin (CK), involucrin (INV), filaggrin (FL)]. F: TAF-related markers FSP, VEGF and Tn-C.

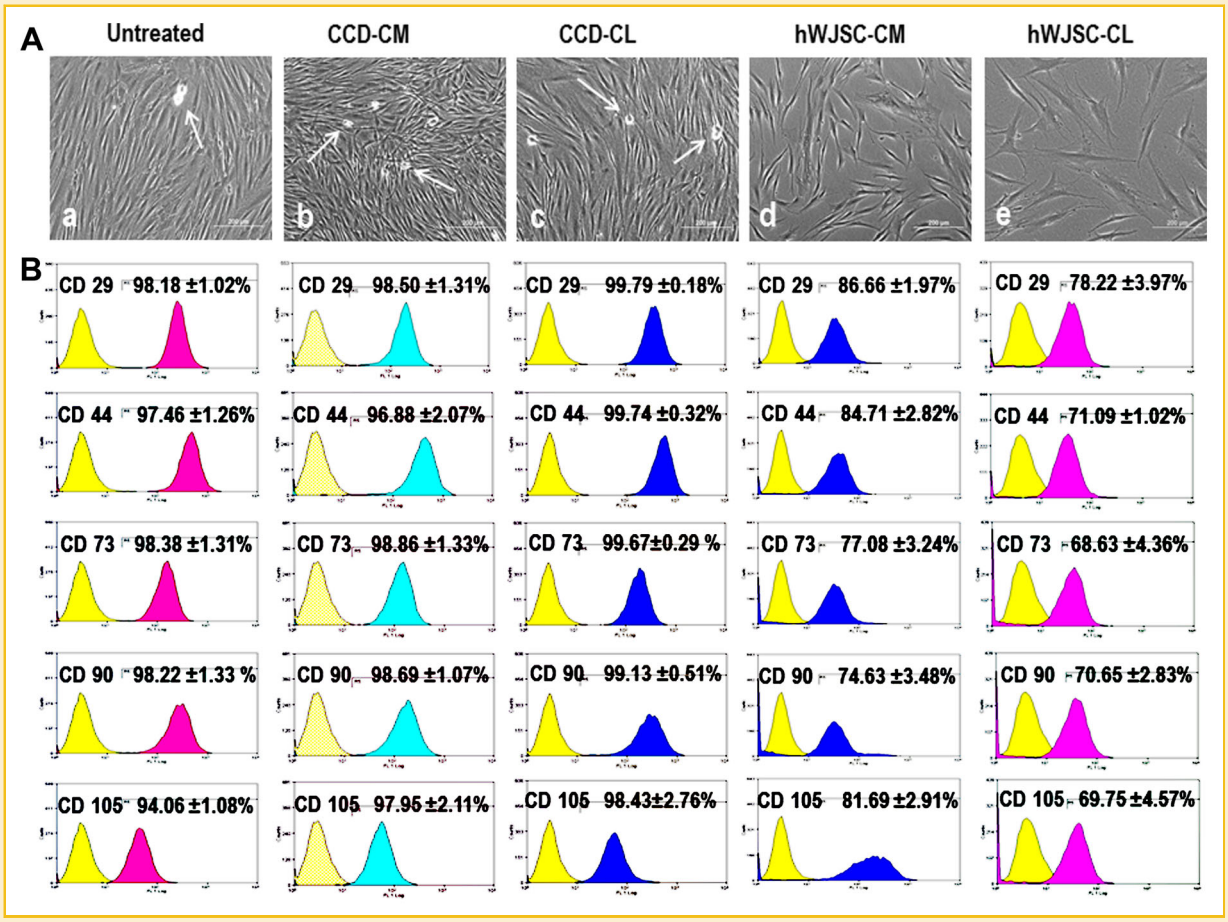

Fig. 2. A: Phase contrast images of morphological changes of human keloid cells exposed to hWJSC-CM and hWJSC-CL. a–c: Note that keloid cells of controls (untreated, CCD-CM, CCD-CL) formed complete confluent monolayers with typical fibroblastic morphology and showed several circular mitotic cells (white arrows) at 72 h. d,e: Keloid cells of treatment dishes exposed to hWJSC-CM and hWJSC-CL at 72 h were not fully confluent, had decreased cell numbers, no mitotic cells, and underwent cell death early. B: The expression of CD markers (CD29, CD44, CD73, CD90, CD105) of keloid cells remained high in controls (Untreated, CCD-CM, CCD-CL) while those of the treatment groups (hWJSC-CM and hWJSC-CL) decreased.

Scratch-wound assay. The keloid cells of the controls (untreated and CCD-CM) migrated from the edges of the scratches and completely covered the vacant areas by Day 2 while the keloid cell migration of hWJSC-CM treated dishes was less and slower with no complete coverage of the scratched areas on Day 2 (Fig. 3A).

Cell proliferation assay. The BrdU assay of keloid cells exposed to hWJSC-CM and hWJSC-CL showed significant decreases in cell proliferation rates on Day 9 compared to controls (Fig. 3B). The mean ± SEM cell proliferation rates were 0.91 ± 0.03 for untreated; 0.92 ± 0.04 for CCD-CM; 0.85 ± 0.01 for CCD-CL; 0.37 ± 0.03 for hWJSC-CM; and 0.59 ± 0.02 for hWJSC-CL. These mean decreases in cell proliferation rates between treatment and control groups were statistically significant (Fig. 3B).

Cell cycle analysis. Keloid cells in untreated control dishes showed normal cell cycle profiles while the keloid cells exposed to the treatments (hWJSC-CM and hWJSC-CL) showed increased peaks in the sub-G1 and G2/M phases compared to their respective controls on Days 3 and 9. The percentage increases for the sub-G1 phase on Day 3 were: hWJSC-CM: 11.18 ± 2.34% and hWJSC-CL: 15.16 ± 3.07% and on Day 9 were: hWJSC-CM: 14.12 ± 1.08% and hWJSC-CL: 11.79 ± 1.53%. For the G2/M phase the percentage increases on Day 3 were: hWJSC-CM: 17.80 ± 1.94% and hWJSC-CL: 18.09 ± 2.74% and on Day 9 were: hWJSC-CM: 19.55 ± 2.37% and hWJSC-CL: 20.73 ± 3.72% (Fig. 4A,B).

Annexin V-FITC assay. Keloid cells treated with hydrogen peroxide (10 mM) for 2–3 h were used as positive control and they showed positive staining for Annexin V-FITC with a lateral shift of the histogram compared to unstained negative controls. Contour plots of keloid cells exposed to hWJSC-CM and hWJSC-CL treatments showed significantly greater mean ± SEM percentages of Annexin V-FITC positive cells compared to controls on both Day 3 (19.75 ± 2.7 to 27.81 ± 2.7 vs. 2.44 ± 1.3 to 6.09 ± 3.4) and on Day 9 (19.08 ± 1.8 to 24.52 ± 2.33 vs. 2.44 ± 1.3 to 6.85 ± 1.1) ($P < 0.05$) (Fig. 5A).

TUNEL assay. Keloid cells were treated with DNAse to act as positive controls to show positive staining for the TUNEL assay. Keloid cells exposed to the treatments (hWJSC-CM and hWJSC-CL) showed positive TUNEL cells compared to controls (Fig. 5B).

Immunocytochemistry. When keloid cells were treated with hWJSC-CM and hWJSC-CL for 72 h their TAF markers stained by immunocytochemistry became weakly positive (Tn-C, FSP, and

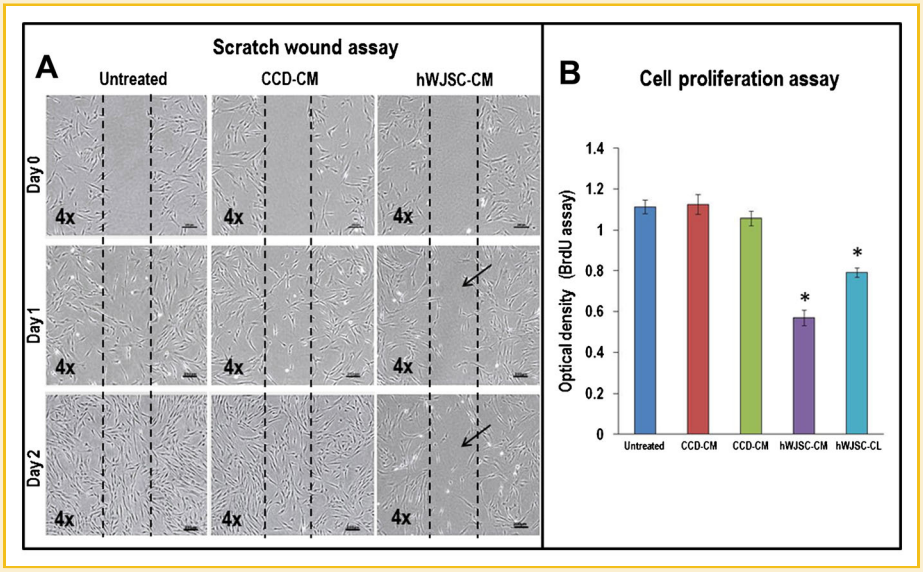

Fig. 3. A: Phase contrast images of scratch-wound assay showing human keloid cells migrating from edges of scratches into vacant areas with complete closure by Day 2 in controls (untreated, CCD-CM) whereas keloid cells of treatment dishes (hWJSC-CM) had slower cell growth, decreased migration, and vacant areas were not fully covered on Day 2 (arrows). B: Histogram shows that cell proliferation (BrDU assay) of human keloid cells were significantly decreased on Day 9 when exposed to hWJSC-CM and hWJSC-CL compared to controls (untreated, CCD-CM, CCD-CL). All values are mean ± SEM from three different replicates $^{*}P < 0.05$.

VEGF) compared to untreated controls (Fig. 6A–C). Also, treated cells showed highly positive immunocytochemical staining for autophagy-related markers (BECLIN- 1 and LC3B) compared to untreated controls (Fig. 7A–B).

Quantitative real time polymerase chain reaction (qRT-PCR). Gene expression analysis using qRT-PCR showed that the anti-apoptotic-related gene SURVIVIN was significantly downregulated and the pro-apoptotic and autophagy-related genes (BAX, ATG5, ATG7, and BECLIN-1) were significantly upregulated in the keloid cells exposed to hWJSC-CM and hWJSC-CL at Day 3 and 9 compared to controls ($P < 0.05$) (Fig. 8Aa–e). The fold decreases in expression levels for the anti-apoptotic-related genes ranged from 0.097 to 0.23 on Day 3 and 0.77 to 0.96 on Day 9 while the fold increases for pro-apoptotic and autophagy-related genes ranged from 0.74 to 6.47 on Day 3 and 5.61 to 53.43 on Day 9. The fold differences for treatments are compared with controls for all genes in Fig. 8Aa–e.

qRT-PCR of the TAF-related genes confirmed the immunocytochemistry results. The TAF genes (TSP, FGF, IL-6, VEGF, FAP, FSP, Tn-C, SMA, SDF-1) were significantly downregulated in keloid cells exposed to hWJSC-CM and hWJSC-CL treatments compared to controls on Days 3 and 9 ($P < 0.05$) (Fig. 8Ba–i).

DISCUSSION

Besides the typical histological features seen in keloid tissues (large fibrillar, glassy collagen bundles, inflammatory cells, and increased extracellular matrix stroma) [Moshref and Mufti, 2010], the characterization results of the present study showed that keloid tissues also contained cells with the typical CD marker signature of mesenchymal stem cells (MSCs) viz., CD29, CD44, CD73, CD90, and CD105. Stem cells from diverse tissues are typically cultured in vitro under adherent conditions in two-dimensional cultures or on three-dimensional matrices or as spheres in suspension culture. Sphere-forming assays evaluate the potential of a cell to behave as a stem cell when removed from its in vivo niche [Pastrana et al., 2011] and have been used conventionally to retrospectively identify stem cell populations. Stem cells from the dermis of skin have been isolated and cultured under sphere-forming conditions by several workers [Toma et al., 2001, 2005; Fernandes et al., 2004]. The ability of the keloid cells in the present study to generate spheres in suspension sphere culture conditions further confirmed the MSC-like nature of keloid cells. Thus, the results of the present study are consistent with the reports of other workers [Moon et al., 2008; Zhang et al., 2009] who showed that keloid tissues contained KPCs or MSC-like cells compared to normal skin. These MSC-like cells when isolated were shown to have high colony-forming capabilities suggestive of the tumor-like nature of keloids [Zhang et al., 2009]. The keloid cells in the present study also showed no decrease in expression of the MSC markers for up to 10 passages in culture suggesting their ability to maintain stemness characteristics for a prolonged period.

It was reported that the secretions of tumor cells could stimulate the movement of host cells from short and long distances from the primary tumor area and this phenomenon takes place throughout tumor growth and metastasis providing the basis for the systemic nature of malignancies [Wels et al., 2008]. Also, the immediate vicinity of the tumor microenvironment contained a wide variety of vascular and stromal cell types that participate in the molecular events leading to tumor invasion and metastasis [Wels et al., 2008]. It was shown that the various cell types in such tumor microenvironments were fibroblasts, endothelial cells, blood cells, and pericytes which interact with the tumor cells via the secretion of cytokines, hormones, chemokines, and proteases [Spaeth et al., 2009]. Those fibroblasts that interact with the tumor cells have been referred to as

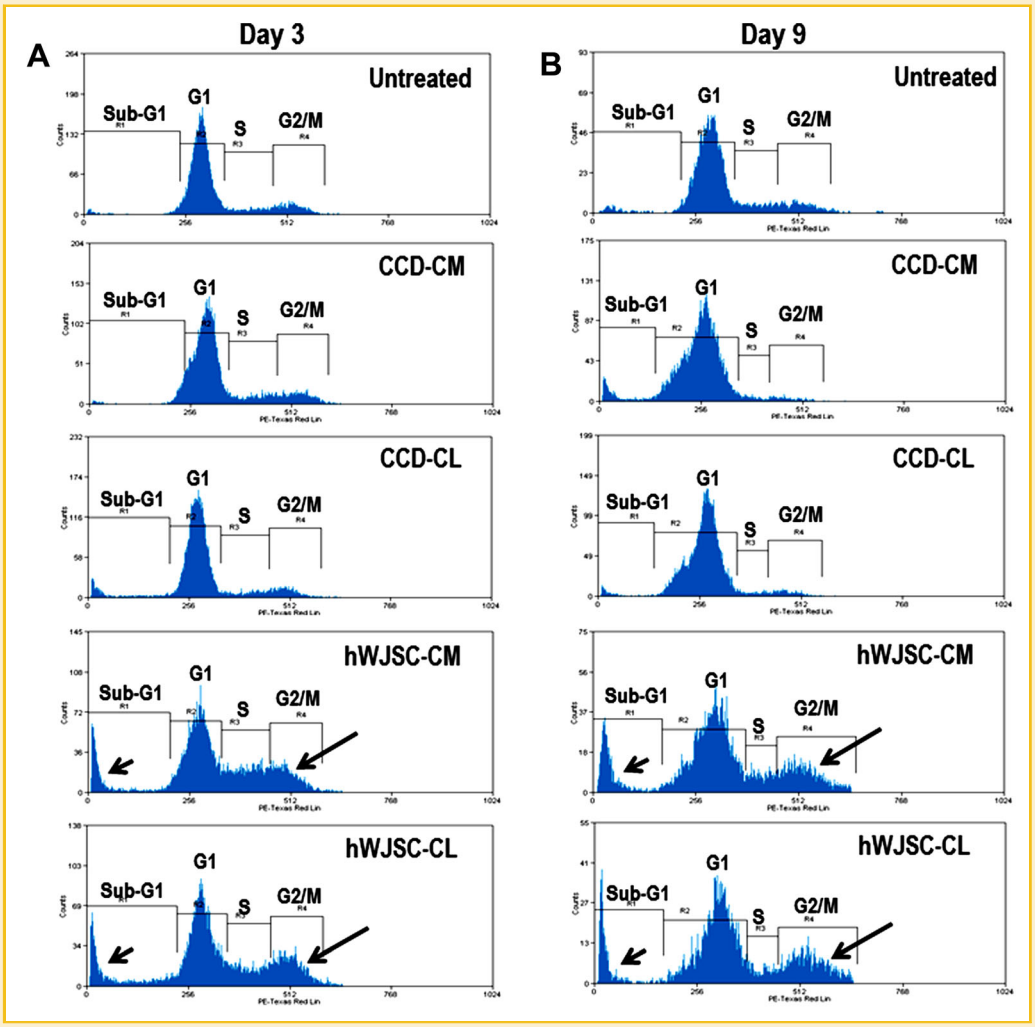

Fig. 4. Cell cycle analysis (Flow cytometry–PI) showing that human keloid cells exposed to treatments (hWJSC–CM and hWJSC–CL) had increased sub–G1 (short arrows) and G2/M (long arrows) phases compared to controls (untreated, CCD–CM, CCD–CL) on Day 3 (A) and Day 9 (B).

tumor-associated fibroblasts (TAF) [Wels et al., 2008] and there is ample evidence to demonstrate that TAFs play an important role in malignant and benign tumor growth particularly for solid tumors [Cardone et al., 1997; Bissell and Radisky, 2001; Blankenstein, 2005]. TAFs can be identified by specific markers such as fibroblast specific protein (FSP), fibroblast activated protein (FCP), cell aggressive markers (tenascin-c, thrombospondin-1, stromelysin-1), tumor growth factors (HGF, EGF, IL-6), and angiogenic factors (alpha smooth muscle actin, desmin, VEGF) [Spaeth et al., 2009]. Some workers reported that TAFs in tumor sites originated from migrating bone marrow derived cells in the peripheral circulation [Jodele et al., 2005] while others later confirmed that these bone marrow derived cells were actually MSCs that had the potential to differentiate into TAFs when in the vicinity of the tumor microenvironment [Spaeth et al., 2009]. The results of the present study demonstrated that keloid cells also carried positive TAF markers further alluding to their MSC-like nature. Hence, taken together, our results demonstrate that keloid scar tissues contain cell populations that are quite unique compared to normal skin fibroblasts, in being highly proliferative and maintaining a normal karyotype with serial passaging, showing distinct MSC and TAF markers with the increased capacity for colony formation. These attributes provide further evidence for their benign tumor-like nature and properties.

Human Wharton's jelly stem cells (hWJSCs) have been shown to have anti-tumorigenic properties against mammary and ovarian adenocarcinoma, osteosarcoma, bladder carinomas, and alveolar-bronchial tumors by several independent groups [Rachakatla et al., 2007; Ayuzawa et al., 2009; Ganta et al., 2009; Maurya et al., 2010; Sun et al., 2010; Ma et al., 2011; Chao et al., 2012; Fonseka et al., 2012; Gauthaman et al., 2012b, 2013; Liu et al., 2013; Wu et al., 2013a]. Cell trafficking occurs during pregnancy between mother and fetus [Herzenberg et al., 1979; Lo et al., 1996] and the fetal cells found in maternal tissues include cells of mesenchymal and hematopoietic origin. Cancer cells can thus cross from the maternal compartment through the placenta to the fetus. However, data from 98 pregnant patients with ovarian carcinomas, breast adenocarcinomas and sarcomas showed placental metastasis in 92% of cases while fetal metastasis was observed in only 17% of the cases. Also,

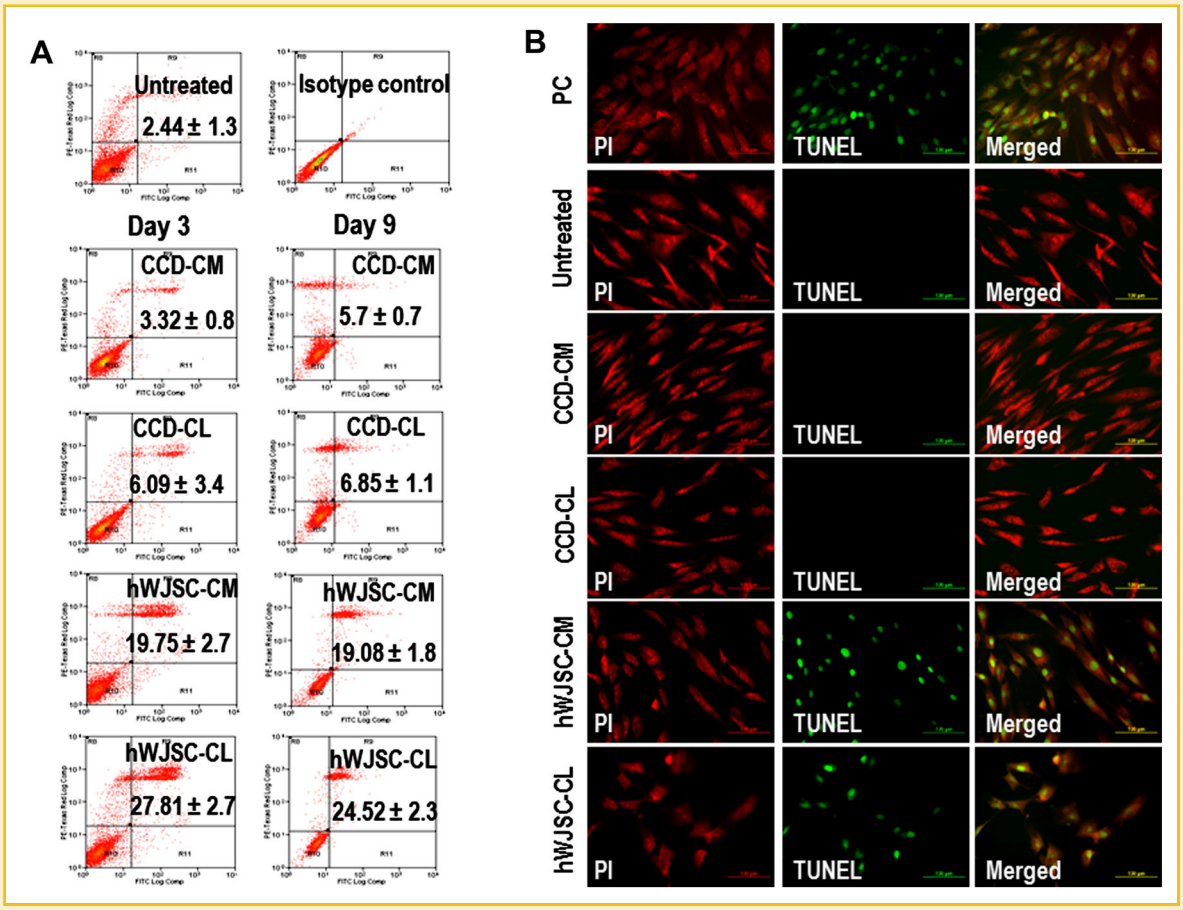

Fig. 5. A: Contour plots (Annexin V-FITC flow cytometry) of human keloid cells showing significantly higher positive cells when exposed to hWJSC-CM and hWJSC-CL compared to controls on Days 3 and 9. Values are mean ± SEM from three different replicates. B: Images of TUNEL-positive human keloid cells when exposed to hWJSC-CM and hWJSC-CL compared to controls (untreated, CCD-CM, CCD-CL). DNAse treated cells were used as positive controls (PC).

choriocarcinoma which is a malignant placental trophoblastic cancer that develops during gestation is usually not observed in the fetus [Liu and Guo, 2006]. It thus appears that besides the placenta there is a more effective defense mechanism in the umbilical cord that blocks the movement of cancer cells from placenta to fetus. Yang and Chao [2013] thus postulated that hWJSCs were gifted with anti-tumorigenic properties to act as a natural guard against cancer cells during movement from mother to fetus via the umbilical cord.

The fact that the percentage expression of the key keloid CD markers (CD29, CD44, CD73, CD90, and CD105) and TAF markers decreased in the presence of hWJSC-CM and hWJSC-CL compared to controls suggests that the stemness and tumorigenic characteristics, self-renewal, and differentiation potential of the keloid cells was altered by anti-tumorigenic agents in the hWJSC-CM and hWJSC-CL. Also, the high percentage of cell death observed in the sub-G1 phase of the cell cycle in hWJSC-CM and hWJSC-CL treated keloid cells indicated that the cells were undergoing apoptosis. The high percentage of Annexin V-FITC positive cells after 3 days of hWJSC-CM and hWJSC-CL treatment also confirmed that the hWJSCs induced keloid cell death. The effect was sustained with a similar percentage of Annexin V positive cells seen after 9 days of the treatment. A larger number of dead cells would have been detected on Day 9 if the floating cells lost during media changes were accounted for on Days 3 and 6. The gene expression profiles showed that the anti-apoptotic-related gene (SURVIVIN) was downregulated and the pro-apoptotic and autophagy-related genes (BAX, ATG5, ATG7, BECLIN-1) were upregulated in the keloid cells exposed to hWJSC-CM and in hWJSC-CL further confirming that the keloid cell death induced by the hWJSCs was via apoptotic and autophagy mechanisms. The high upregulation of TAF markers in keloid cells exposed to CCD-CM (up to 80-fold increase) suggests that the skin might be a natural breeding ground for keloid cells.

The mechanisms of the anti-tumorigenic properties of hWJSCs was reported to be due to cell-to-cell contact and non-contact mechanisms where cell inhibition was via bioactive soluble molecules secreted by the hWJSCs into the neighboring environment [Maurya et al., 2010; Chao et al., 2012; Bongso and Fong, 2013]. Keloid cell fibroblasts were shown to induce MSC chemoattraction towards them in cell migration assays while normal fibroblasts failed to be chemoattracted to keloid cells [Akino et al., 2008]. hWJSCs were shown to release at least four families of bioactive molecules in high concentrations into hWJSC-CM and hWJSC-CL viz., glycosoamino-glycans (GAGs), cytokines, cell adhesion molecules, and growth factors [Fong et al., 2012]. Of these molecules, IGF-1 was shown to

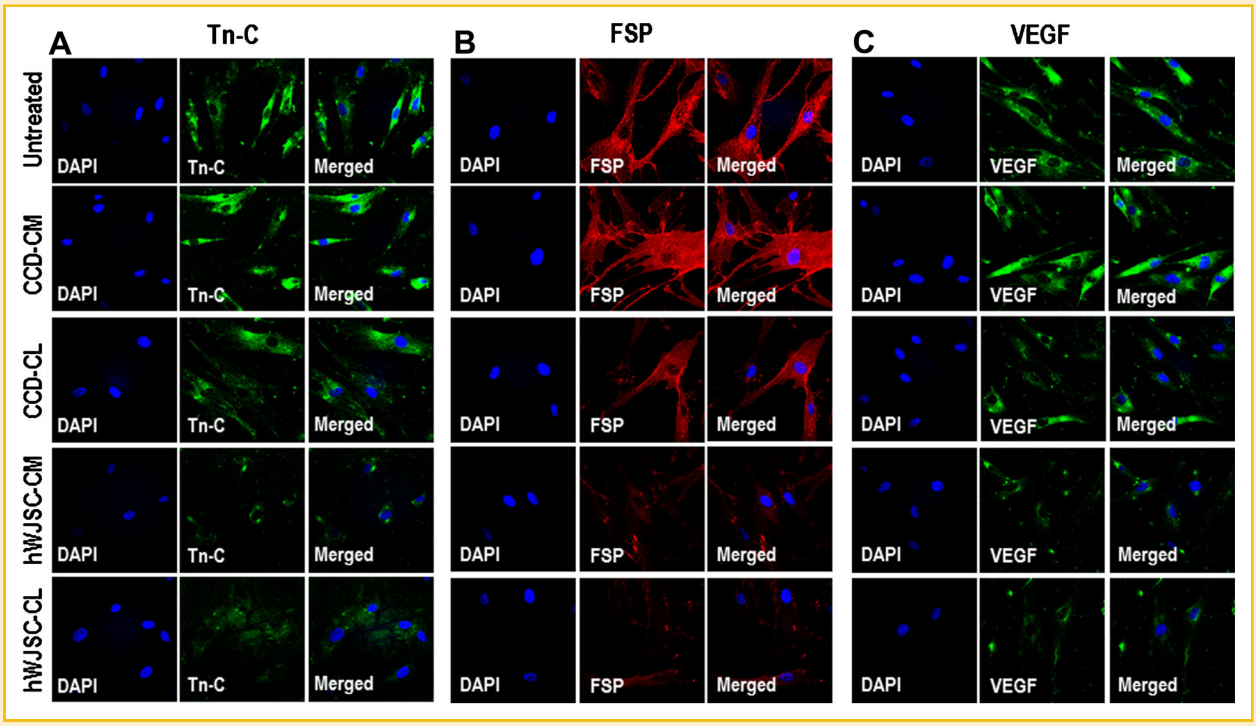

Fig. 6. Immunocytochemistry images showing weakly positive TAF-related markers (A) Tn-C, (B) FSP, and (C) VEGF in human keloid cells exposed to hWJSC-CM and hWJSC-CL compared to controls (untreated, CCD-CM, CCD-CL).

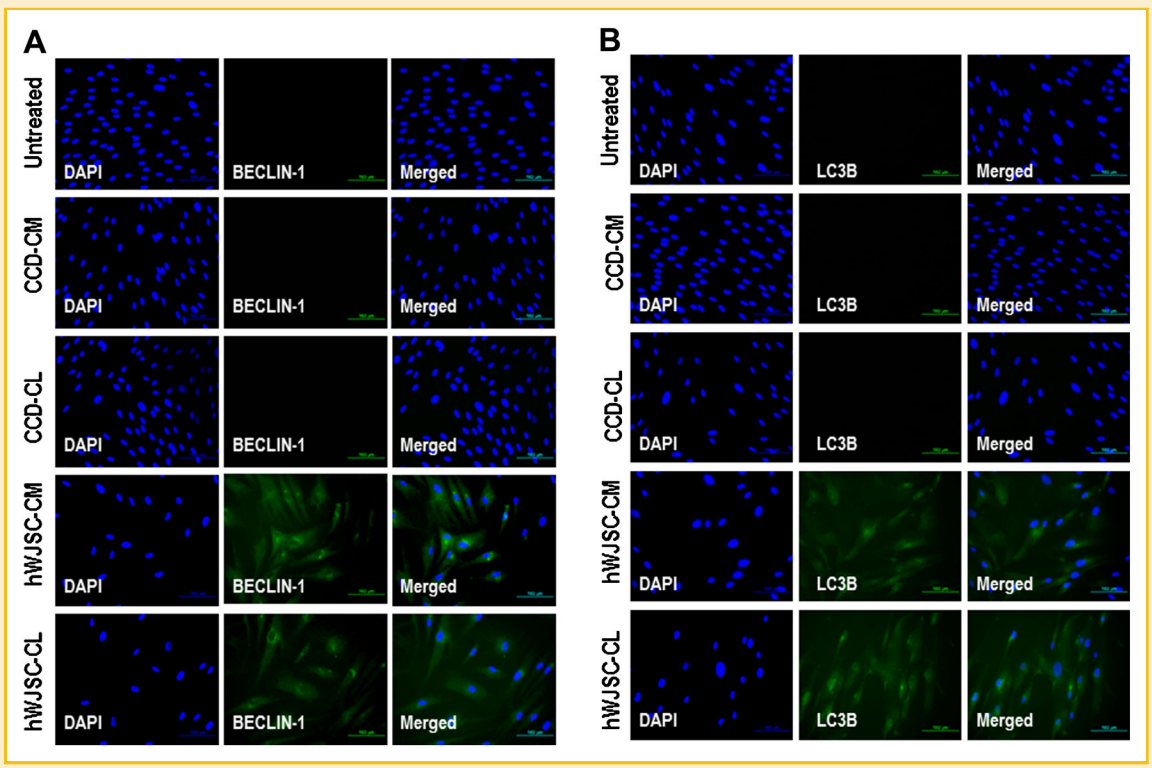

Fig. 7. Immunohistochemistry images of human keloid cells exposed to hWJSC-CM and hWJSC-CL showing positive staining for (A) BECLIN-1 and (B) LC3B compared to controls (untreated, CCD-CM, CCD-CL).

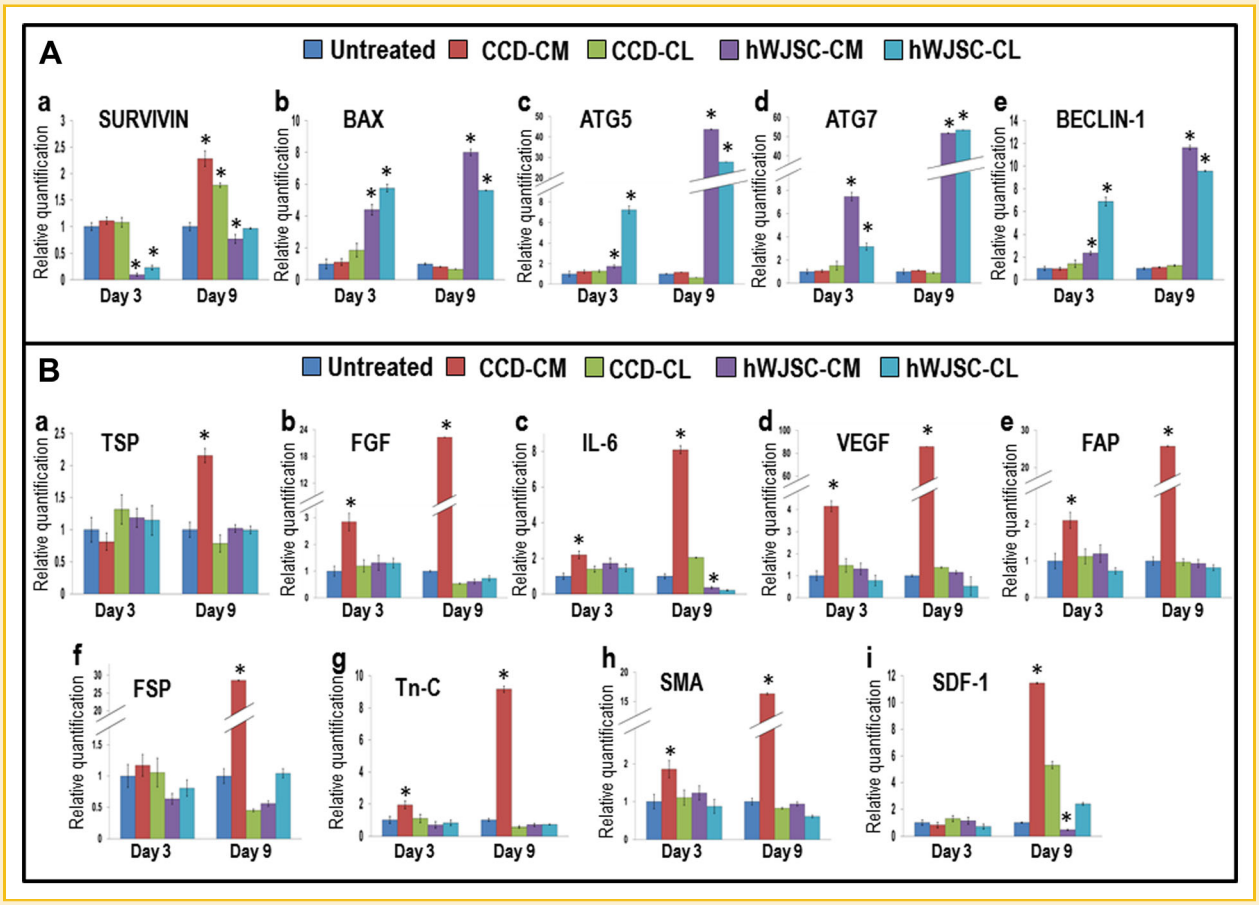

Fig. 8. A: Gene expression profiles (qRT-PCR) showing downregulation of the anti-apoptotic-related genes (SURVIVIN) and upregulation of the pro-apoptotic and autophagy-related genes (BAX, ATG5, ATG7, and BECLIN-1) in human keloid cells exposed to hWJSC-CM and hWJSC-CL compared to controls (untreated, CCD-CM, CCD-CL) ($P < 0.05$). B: qRT-PCR showing upregulation of TAF-related genes (TSP, FGF, IL-6, VEGF, FAP, FSP, Tn-C, SMA, SDF-1) in human keloid cells exposed to hWJSC-CM and hWJSC-CL compared to controls (untreated, CCD-CM, CCD-CL) ($P < 0.05$). Data analysis and relative quantitation was done using the comparative Ct (DDCt) method.

play an important role in the pathogenesis of keloids [Akino et al., 2008]. It was also suggested that the increased fibroblast proliferative activity in keloid tissues may normalize if the cytokine milieu surrounding the keloid is manipulated [Ehrlich et al., 1994; Szulgit et al., 2002; Moon et al., 2008]. Hence modulation of the production of these molecules may provide useful treatments for keloids.

Since Interleukin (IL)-10 is an anti-inflammatory and antifibrotic cytokine and in the embryo it is important for scarless wound repair, Kieran et al. [2013] recently investigated its effect on scarring of wounds in a knockout (KO) mouse model carrying double deletion of the IL-10 and IL-4 genes and also the effect of exogenous addition of recombinant human (rh) IL-10 into rat and human cutaneous incisions. Their results showed that the KO mice healed with poor scar histology and increased inflammation while rhIL-10-treated rat incisions healed with decreased inflammation, better scar histology, and better macroscopic scar appearance. The rhIL-10-treated human incisions at low concentrations healed with better macroscopic scar appearance and less red scars. They concluded that IL-10 was an important cytokine in wound healing and suppression of inflammation and scarring.

The results of the present study suggest that hWJSCs and hWJSC-CM alter the nature of the benign tumorigenicity of keloid cells making them lose their neoplastic features and becoming non-invasive. In pilot studies we observed that specific miRNA clusters (miR-106a-363, miR-17-92, miR-106b-25, miR-302-367, miR-21, miR-34a, and the let-7 family) were highly expressed in hWJSCs. The miR-106a-363 and miR-17-92 clusters are involved in cell proliferation and growth thus possibly playing a role in the wound healing process and miR-34a and the let-7 family are involved in anticancer processes. Thus, future studies should be aimed at evaluating the anti-keloid properties of the proteins released by these specific miRNAs. Such potential proteins will also be of tremendous therapeutic value in the future treatment of keloids.

ACKNOWLEDGMENTS

The authors acknowledge the grant support to carry out this work from the Academic Research Fund, National University of Singapore (AcRF-NUS) (R-174-000-129-112) and the National Medical Research Council (NMRC) (R-174-000-131-213).

REFERENCES

Akino K, Akita S, Yakabe A, Mineda T, Hayashi T, Hirano A. 2008. Human mesenchymal stem cells may be involved in keloid pathogenesis. Int J Dermatol 47:1112–1117.

Ayuzawa R, Doi C, Rachakatla RS, Pyle MM, Maurya DK, Troyer D. 2009. Naïve human umbilical cord matrix derived stem cells significantly attenuate growth of human breast cancer cells in vitro and in vivo. Cancer Lett 280:31–37.

Bissell MJ, Radisky D. 2001. Putting tumors in context. Nat Rev Cancer 1:46–54.

Blankenstein T. 2005. The role of tumor stroma in the interaction between tumor and immune system. Curr Opin Immunol 17:180–186.

Blit PH, Jeschke MG. 2012. Keloids: What do we know and what do we do next? Transl Res 159:173–174.

Bongso A, Fong CY. 2013. The therapeutic potential, challenges and future clinical directions of stem cells from the Wharton′s jelly of the human umbilical cord. Stem Cell Rev 9:226–236.

Cardone A, Tolino A, Xarcone R, Borruto Caracciolo G, Tartaglia E. 1997. Prognostic value of desmoplastic reaction and lymphocytic infiltration in the management of breast cancer. Panminerva Med 39:174–177.

Chao KC, Chao KF, Fu YS, Liu SH. 2008. Islet-like clusters derived from mesenchymal stem cells in Wharton′s jelly of the human umbilical cord for transplantation to control type 1 diabetes. PLoS ONE e1451:1–9.

Chao KC, Yang HT, Chen MW. 2012. Human umbilical cord mesenchymal stem cells suppress breast cancer tumorogenesis through direct cell-cell contact and internalization. J Cell Mol 16:1803–1815.

Chen H, Zhang NK, Lia TC, Guo JW, Wang ZG, Yang M, Gao LR. 2012. Human umbilical cord Wharton′s jelly stem cells: Immune property genes assay and effect of transplantation on the immune cells of heart failure patients. Cell Immunol 276:83–90.

Cory G. 2011. Scratch-wound assay. Methods Mol Biol 769:25–30.

Ehrlich HP, Desmouliere A, Diegelmann RF, Cohen IK, Compton CC, Garner WL, Kapanci Y, Gabbiani G. 1994. Morphological and immunochemical differences between keloid and hypertrophic scar. Am J Pathol 145:105–113.

Estes JM, Adzick NS, Harrison MR, Longaker MT, Stern R. 1993. Hyaluronate metabolism undergoes an ontogenic transition during fetal development: Implications for scar-free wound healing. J Pediatr Surg 28:1227–1231.

Fan CG, Zhang Q, Zhou J. 2011. Therapeutic potentials of mesenchymal stem cells derived from human umbilical cord. Stem Cell Rev Rep 7:195–207.

Fernandes KJ, McKenzie IA, Mill P, Smith KM, Akhavan M, Barnabé-Heider F, Biernaskie J, Junek A, Kobayashi NR, Toma JG, Kaplan DR, Labosky PA, Rafuse V, Hui CC, Miller FD. 2004. A dermal niche for multipotent adult skin-derived precursor cells. Nat Cell Biol 6:1082–1093.

Fong CY, Chak LL, Biswas A, Tan JH, Gauthaman K, Chan WK, Bongso A. 2011. Human Wharton′s jelly stem cells have unique transcriptome profiles compared to human embryonic stem cells and other mesenchymal stem cells. Stem Cell Rev Rep 7:1–16.

Fong CY, Gauthaman K, Cheyyatraivendran S, Lin HD, Biswas A, Bongso A. 2012. Human umbilical cord Wharton′s jelly stem cells and its conditioned medium support hematopoietic stem cell expansion ex vivo. J Cell Biochem 113:658–668.

Fong CY, Subramanian A, Biswas A, Gauthaman K, Srikanth P, Hande P, Bongso A. 2010. Derivation efficiency, cell proliferation, frozen-thaw survival, 'stemness' properties, and differentiation of human Wharton′s jelly stem cells: Their potential for concurrent banking with cord blood for regenerative medicine purposes. Reprod Biomed Online 21:391–401.

Fonseka M, Ramasamy R, Yip WK, Tan BC, Seow HF. 2012. Human umbilical cord blood-derived mesenchymal stem cells (hUCB-MSC) inhibits the proliferation of K562 (Human erythromyeloblastoid leukemic cell line). Cell Biol Int 36:793–801.

Ganta C, Chiyo D, Ayuzawa R, Rachakatla R, Pyle M, Andrews G, Weiss M, Tamura M, Troyer D. 2009. Rat umbilical cord stem cells completely abolish rat mammary carcinomas with no evidence of metastasis or recurrence 100 days post-tumor cell inoculation. Cancer Res 69:1815–1820.

Gauglitz GG, Korting HC, Pavicic T, Ruzicka T, Jeschke MG. 2011. Hypertrophic scarring and keloids: Pathomechanims and current and emerging treatment strategies. Mol Med 17:113–125.

Gauglitz GG. 2013. Management of keloids and hypertrophic scars: Current and emerging options. Clin Cosmet Investig Dermatol 6:103–114.

Gauthaman K, Fong CY, Arularasu S, Subramanian A, Biswas A, Choolani M, Bongso A. 2013. Human Wharton′s Jelly stem cell conditioned medium and cell-free lysate inhibit human osteosarcoma and mammary carcinoma cell growth in vitro and in xenograft mice. J Cell Biochem 114:366–377.

Gauthaman K, Fong CY, Suganya CA, Subramanian A, Biswas A, Choolani M, Bongso A. 2012a. Extra-embryonic human Wharton′s jelly stem cells do not induce tumorigenesis, unlike human embryonic stem cells. Reprod Biomed Online 24:235–246.

Gauthaman K, Fong CY, Cheyyatraivendran S, Biswas A, Choolani M, Bongso A. 2012b. Human umbilical cord Wharton′s jelly stem cell (hWJSC) extracts inhibit cancer cell growth in vitro. J Cell Biochem 113:2027–2039.

Gauthaman K, Venugopal JR, Fong CY, Biswas A, Ramakrishna S, Bongso A. 2011. Osteogenic differentiation of human Wharton′s jelly stem cells on nanofibrous substrates in vitro. Tissue Eng Part A 17:71–81.

Herzenberg LA, Bianchi DW, Schroder J. 1979. Fetal cells in the blood of pregnant women: Detection and enrichment by fluorescence-activated cell sorting. Proc Natl Acad Sci USA 76:1453–1455.

Iqbal SA, Sidgwick GP, Bayat A. 2012. Identification of fibrocytes from mesenchymal stem cells in keloid tissue: A potential source of abnormal fibroblasts in keloid scarring. Arch Dermatol Res 304:665–671.

Jodele S, Chantrain CF, Blavier I, Lutzko C, Crooks GM, Shimada H. 2005. The contribution of bone marrow derived cells to the tumor vasculature in neuroblastoma is matrix metalloproteinase 9 dependent. Cancer Res 65:3200–3208.

Kieran I, Knock A, Bush J, So K, Metcalfe A, Hobson R, Mason T, O′Kane s, Ferguson M. 2013. Interleukin-10 reduces scar formation in both animal and human cutaneous wounds: Results of two preclinical and phase II randomized control studies. Wound Repair Regen 3:428–436.

La Rocca G, Anzalone R, Corrao S, Magno F, Loria T, Lo Iacono M. 2009. Isolation and characterization of OCT4 +/HLA-G+ mesenchymal stem cells from the human umbilical cord matrix: Differentiation potential and detection of new markers. Histochem Cell Biol 131:267–282.

Liu J, Guo L. 2006. Intraplacental choriocarcinoma in a placenta with both maternal and infantile metastases: A case report and review of the literature. Gynecol Oncol 103:1147–1151.

Liu J, Han G, Liu H, Qin C. 2013. Suppression of cholangiocarcinoma cell growth by human umbilical cord mesenchymal stem cells: A possible role of Wnt and Akt signaling. PLoS ONE 8:e62844.

Lo YM, Lo ES, Watson N, Noakes L, Sargent IL, Thilaganathan B, Wainscoat JS. 1996. Two-way cell traffic between mother and fetus: Biologic and clinical implications. Blood 88:4390–4395.

Lorenz HP, Longaker MT, Perkocha LA, Jennings RW, Harrison MR, Adzick NS. 1992. Scarless wound repair: A human fetal skin model. Development 114:253–259.

Ma Y, Hao X, Zhang S, Zhang J. 2011. The in vitro and in vivo effects of human umbilical cord mesenchymal stem cells on the growth of breast cancer cells. Breast Cancer Res Treat 133:473–485.

Mansilla E, Marin GH, Sturla F, Drago HE, Gil MA, Salas E, Gardiner MC, Piccinelli G, Bossi S, Salas E, Petrelli L, Iorio G, Ramos CA, Soratti C. 2005. Human mesenchymal stem cells are tolerized by mice and improve skin and spinal cord injuries. Transplant Proc 37:292–294.

Maurya DK, Doi C, Kawabata A, Pyle MM, King C, Wu Z, Troyer D, Tamura M. 2010. Therapy with un-engineered naïve rat umbilical cord matrix stem cells markedly inhibits growth of murine lung adenocarcinoma. BMC Cancer 10:590–600.

Mogili NS, Krishnaswamy VR, Jyaraman M, Rajaram R, Venkatraman A, Korrapati PS. 2012. Altered angiogenic balance in keloids: A key to therapeutic intervention. Transl Res 159:182–189.

Moon JH, Kwak SS, Park G, Jung HY, Yoon BS, Park J, Ryu KS, Choi SC, Maeng I, Kim B, Jun EK, Kim S, Kim A, Oh S, Kim H, Kim KD, You S. 2008. Isolation and characterization of multipotent human keloid-derived mesenchymal-like stem cells. Stem Cells Dev 17:713–724.

Moshref SS, Mufti ST. 2010. Keloid and hypertrophic scars: Comparative histopathologocal and immunohistochemical study. JKAU: Med Sci 17:3–22.

Nekanti U, Rao VB, Bahirvani AG, Jan M, Totey S, Ta M. 2010. Long-term expansion and pluripotent marker array analysis of Wharton′s jelly-derived mesenchymal stem cells. Stem Cells Dev 19:117–130.

Pappa KI, Anagnou NP. 2009. Novel sources of fetal stem cells: Where do they fit on the developmental continuum? Future Med 4:423–433.

Pastrana E, Silva-Vargas V, Doetsch F. 2011. Eyes wide open: A critical review of sphere-formation as an assay for stem cells. Cell Stem Cell 8:486–498.

Prasanna SJ, Jahnavi VS. 2011. Wharton′s jelly mesenchymal stem cells as off-the-shelf cellular therapeutics: A closer look into their regenerative and immunomodulatory properties. Open Tiss Eng Reg Med 4:28–38.

Rachakatla RS, Marini F, Weiss ML, Tamura M, Troyer D. 2007. Development of human umbilical cord matrix stem cell-based gene therapy for experimental lung tumors. Cancer Gene Ther 14:828–835.

Rao MS, Mattson MP. 2001. Stem cells and aging: Expanding the possibilities. Mech Ageing Dev 122:713–734.

Seshareddy K, Troyer D, Weiss ML. 2008. Methods to isolate mesenchymal-like cells from Wharton′s jelly of umbilical cord. Methods Cell Biol 86:101–119.

Spaeth EK, Dembiski JL, Sasser AK, Watson K, Klopp A, Hall B. 2009. Mesenchymal stem cell transition to tumor-associated fibroblasts contributes to fibrovascular network expansion and tumor progression. PLoS ONE 4: e49921-11.

Sudo K, Kanno M, Miharada K, Ogawa S, Hiroyama T, Saijo K, Nakamura Y. 2007. Mesenchymal progenitors able to differentiate into osteogenic, chondrogenic, and/or adipogenic cells in vitro are present in most primary fibroblast-like cell populations. Stem Cells 25:1610–1617.

Sun B, Yu KR, Bhandari DR, Jung JW, Kang SK, Kang KS. 2010. Human umbilical cord blood mesenchymal stem cell-derived extracellular matrix prohibits metastatic cancer cell MDA-MB-231 proliferation. Cancer Lett 296:178–185.

Szulgit G, Rudolph R, Wandel A, Tenenhaus M, Panos R, Gardner H. 2002. Alterations in + broblast alpha1beta1 integrin collagen receptor expression in keloids and hypertrophic scars. J Invest Dermatol 118:409–415.

Taghizadeh RR, Cetrulo KJ, Cetrulo CL. 2011. Wharton′s jelly stem cells: Future clinical applications. Placenta 32:S311–S315.

Toma JG, Akhavan M, Fernandes KJL, Barnabe-Heider F, Sadikot A, Kaplan DR, Miller FD. 2001. Isolation of multipotent adult stem cells from the dermis of mammalian skin. Nat Cell Biol 3:778–784.

Toma JG, McKenzie IA, Bagli D, Miller FD. 2005. Isolation and characterization of multipotent skin-derived precursors from human skin. Stem Cells 23:727–737.

Troyer DL, Weiss ML. 2008. Concise review: Wharton′s jelly-derived cells are a primitive stromal cell population. Stem Cells 26:591–599.

Walter MN, Wright KT, Fuller HR, MacNeil S, Johnson WE. 2010. Mesenchymal stem cell-conditioned medium accelerates skin wound healing: An in vitro study of fibroblast and keratinocyte scratch assays. Exp Cell Res 316:1271–1281.

Wang XY, lan Y, He WY, Zhang L, Yao HY, Hou C, Tong Y, Liu YL, Yang G, Liu XD, Yang X, Liu B, Mao N. 2008. Identification of mesenchymal stem cells in aorta-gonad-mesonephros and yolk sac of human embryos. Blood 111:2436–2443.

Wang Y, Han ZB, Ma J, Zuo C, Geng J, Gong W, Sun Y, Li H, Bin Wang, Zhang L, He Y, Han ZC. 2012. A toxicity study of multiple-administration human umbilical cord mesenchymal stem cells in cynomolgus monkeys. Stem Cells Dev 21:1401–1408.

Wels J, Kaplan RN, Rafii S, Lyden D. 2008. Migratory neighbors and distant invaders: Tumor associated niche cells. Genes Dev 22:559–574.

Wu S, Ju GQ, Du T, Zhu YJ, Liu GH. 2013a. Microvesicles derived from human umbilical cord wharton′s jelly mesenchymal stem cells attenuate bladder tumor cell growth in vitro and in vivo. PLoS ONE 8:e61366.

Wu KH, Tsai C, Wu HP, Sieber M, Peng CT, Chao YH. 2013b. Human application of ex-vivo expanded umbilical cord-derived mesenchymal stem cells: Enhance hematopoiesis after cord blood transplantation. Cell Tranplant 22:2041–2051.

Zhang Q, Yamaza T, Kelly AP, Shi S, Wang S, Brown J, Wang L, French SW, Shi S, Le AD. 2009. Tumor-like stem cells derived from human keloid are governed by the inflammatory niche driven by IL-17/IL-6 axis. PLoS ONE 4:e7798.

Yang HT, Chao KC. 2013. Foetal defence against cancer: A hypothesis. J Cell Mol Med 17:1096–1098.